NASA TECHNICAL NOTE

NASA TN D-4568

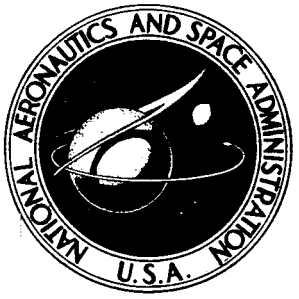

NASA TN D-4568

PENETRATION RESISTANCE OF DOUBLE-SHEET STRUCTURES AT VELOCITIES TO 8.8 KM/SEC

by C. Robert Nysmith

Ames Research Center

Moffett Field, Calif.

NATIONAL AERONAUTICS AND SPACE ADMINISTRATION • WASHINGTON, D. C. • MAY 1968

NASA TN D-4568

PENETRATION RESISTANCE OF DOUBLE-SHEET STRUCTURES AT VELOCITIES TO 8.8 KM/SEC

By C. Robert Nysmith

Ames Research Center
Moffett Field, Calif.

NATIONAL AERONAUTICS AND SPACE ADMINISTRATION

For sale by the Clearinghouse for Federal Scientific and Technical Information
Springfield, Virginia 22151 – CFSTI price $3.00

PENETRATION RESISTANCE OF DOUBLE-SHEET STRUCTURES AT VELOCITIES TO 8.8 KM/SEC

By C. Robert Nysmith

Ames Research Center

SUMMARY

Small pyrex glass spheres were launched into aluminum double-sheet targets at velocities to 8.8 km/sec to determine the effects of total sheet thickness and sheet spacing upon penetration resistance. The ballistic limit of double-sheet structures consisting of two equally thick aluminum sheets was found to increase with increasing total sheet thickness and sheet spacing. In addition, for a particular ratio of total sheet thickness to projectile diameter, the effectiveness of sheet spacing increases with increasing impact velocity. This effect is attributed to melting and vaporization of the projectile and front-sheet material, and it is concluded that this trend will continue as material vaporization becomes more dominant. The data of this report are used to establish the effectiveness of total sheet thickness and a lower limit for the effectiveness of sheet spacing. It was determined that the structural ballistic limit varies with the 2.5 power of the ratio of the total sheet thickness to the projectile diameter and with at least the square of the ratio of the sheet spacing to the projectile diameter.

The data indicate that for impacts at a given velocity the ratio of front-sheet thickness to projectile diameter that causes maximum vaporization or fragmentation or both will result in the most efficient meteor bumper. It is concluded that the double-sheet structure most efficient in resisting penetration will use that thickness for a front sheet and the remaining available mass in the rear sheet.

Measurements were also made of the front-sheet hole diameter and the front-sheet mass loss. It was determined that the front-sheet hole diameter varies with the square root of the impact velocity and the 0.45 power of the front-sheet thickness and the front-sheet mass loss varies with impact velocity and the square of the front-sheet thickness.

INTRODUCTION

The impact resistance of composite structures is being studied at the Ames Research Center. A portion of this investigation, concerned with the penetration resistance of aluminum double-sheet structures at velocities to 7.3 km/sec (ref. 1), indicated that impact results obtained at low speeds are not applicable at high speeds. Consequently, it was concluded that if a structure is to be assessed for its resistance to meteoroid impact, it should be tested at the highest velocity attainable. With this in mind, the aluminum

double-sheet target impact results were extended to an impact velocity of 8.8 km/sec. The purpose of this report is to present these results and to evaluate the effects of total target thickness and sheet spacing upon target penetration resistance.

NOTATION

B.L.	ballistic limit
D	diameter of hole in front sheet
d	projectile diameter
h	sheet spacing
ΔM	front-sheet mass loss
m	projectile mass
t_T	total sheet thickness
t_1	front-sheet thickness
v	impact velocity

EXPERIMENTAL PROCEDURE

Small projectiles were launched from the Ames impact-range light-gas gun into double-sheet targets at velocities to 8.8 km/sec. The range configuration is illustrated in figure 1, and the gun is described in detail in reference 2. The projectiles were 3.2-mm-diameter pyrex glass spheres with a density of 2.23 gm/cm^3. They were mounted in supporting sabots which guided them down the bore of the gun barrel and protected them from the propellant gases. After launch, depending upon whether a smooth-bore or rifled barrel was used, the sabots were aerodynamically or spin separated, respectively, and were deflected in the blast-tank portion of the range to prevent them from impacting the targets.

The spheres continued to fly through the flight chamber, which was instrumented with six spark shadowgraph stations, each presenting two orthogonal views of the projectile in flight. Two stations were equipped with Kerr-cell shutters with exposure times of about 5 nsec so that the structural integrity of the model could be accurately determined. Time intervals were recorded on 10- and 100-mc counter chronographs, and the measurements of time and distance gave projectile velocities accurate within 1.0 percent.

Each target consisted of two sheets of 2024-T3 aluminum spaced a known distance apart. The total target thicknesses tested were 3.2, 4.1, 4.6, 5.1,

and 6.4 mm, and the sheet spacing (distance between the front and rear sheets) varied from 9.5 to 38.1 mm. In all tests, the front and rear sheets were equal in thickness. In addition, all targets were placed normal to the projectile trajectory, at zero stress level, and at room temperature when impact occurred. The ambient pressure in the range varied from 34 to 77 mm Hg of nitrogen when the sabots were aerodynamically separated; the pressure was about 2 mm Hg of air when the sabots were spin separated.

RESULTS AND DISCUSSION

Effect of Target Sheet Thickness and Sheet Spacing

The penetration resistance of each structure was assessed by determining its "ballistic limit," defined in reference 1 as "the projectile velocity required to damage the rear sheet of a structure so that it will no longer hold a pressure difference of one atmosphere without leaks." It has been noted that this criterion does not differentiate between failures due to individual spray particle craters and those resulting from cracks and spalls produced by the concerted action of the fragmented, melted, and vaporized particles striking the sheet. However, for impacts within the meteoric velocity range and for realistic sheet thicknesses, projectile fragmentation will surely be complete and the ballistic-limit criterion should define the penetration resistance of a structure to meteoroid impact.

To establish the ballistic limit of a particular structure, shots must be made at velocities both greater and less than the ballistic limit. The accuracy of the ballistic limit, therefore, depends upon obtaining launch speeds near a desired velocity. For the results presented here, the ballistic limit is generally determined within 7 percent.

The effects of total sheet thickness and sheet spacing upon the penetration resistance of double-sheet structures are shown in figure 2, where the ballistic limit is plotted versus the ratio of sheet spacing to projectile diameter, h/d, for the various ratios of total sheet thickness to projectile diameter, t_T/d. The data of reference 1 are included as the closed symbols; it should be noted that the data point labeled P has been determined more accurately by additional tests in the present test program and indicates a ballistic limit somewhat lower than presented in reference 1. The impact velocities that bracket the ballistic limit of a structure are represented by the error bars associated with each configuration. However, for several structures tested, the impact velocities attainable were too low to cause failure as defined in this report. The small arrows associated with three of the structures in figure 2 indicate this situation.

In reference 1, it was shown that when glass spheres impact aluminum double-sheet targets at low velocities, the projectile and front-sheet spray material form a tight cluster of large fragments that tends to punch a hole in the rear sheet. In this impact regime (defined as the low-speed impact region), the target ballistic limit varies with the 0.25 power of the sheet spacing and the first power of the total sheet thickness (fig. 2). On the

other hand, when impact occurs at high velocities, the projectile and front-sheet spray material are fragmented into an expanding hemispherically shaped cloud of relatively small particles. These particles strike the rear sheet, and rear-sheet failure is characterized by spallation and cracks that radiate outward from the center of the damaged area. This regime is defined as the high-speed impact region. There is a transition region where the projectile breakup process is changing from that of the low-speed case to that of the high-speed case, and rear-sheet damage varies accordingly. It is clear that these impact regions are relative and that the velocities defining the regions vary with projectile and target material as well as target thickness. Consequently, these regions of impact should be considered as "regimes of bumper effectiveness" rather than "velocity regimes."

In figure 2, for impacts at velocities greater than 5.5 km/sec, the ballistic limit increases as both t_T/d and h/d increase. Moreover, the relative effectiveness of spacing increases with increasing velocity over virtually the entire test range. This effect arises because fragmentation and vaporization of the projectile and front-sheet spray material increases with increasing impact velocity, which in turn results in a more favorable distribution of this material over a large area of the rear sheet. The effect of impact velocity, illustrated in figure 3 by photographs of the rear-sheet damage for $t_T/d = 1.0$, is characterized by the size of the craters in the rear sheet and by melting and vaporization; the lateral extent of the damaged area should be ignored since it is primarily the result of the sheet spacing not being the same for the several targets shown in figure 3. For $t_T/d = 1.0$, an impact velocity of 5.65 km/sec fragments the front-sheet spray material into relatively large solid particles that impact the rear sheet and produce the type of damage shown in figure 3(a). As the impact velocity increases to about 7.2 km/sec, the spray material fragments into smaller and smaller particles and the craters in the rear sheet become smaller and occur in relatively orderly rings (figs. 3(b) through (e)). At an impact velocity of about 7.8 km/sec, melting and vaporization begin to occur, and rear-sheet damage is as shown in figure 3(f). As the impact velocity is increased to 8.34 km/sec (the highest velocity of this test), melting and vaporization become more complete (figs. 3(g) and (h)) and the damage is more uniformly distributed over the rear sheet. Melting and vaporization will surely become more complete as the impact velocity increases above that of these tests. Consequently, the effectiveness of sheet spacing for penetration resistance should be considerably greater for impacts at meteoroid velocities into thin front sheets.

On the other hand, target thickness, particularly front-sheet thickness, also has a large effect upon material vaporization. This effect is illustrated in figure 4 by comparing the variation in the type of rear-sheet damage produced by front sheets of different thicknesses impacted at approximately the same impact velocity. Once again, the sheet spacing effects the extent of the areas of damage to the rear sheets. It is seen that for the thickest front sheet of this test ($t_1/d = 1.0$ corresponding to $t_T/d = 2.0$) the spray particles are quite large and produce large individual craters in the rear sheet (fig. 4(a)). As the front-sheet thickness decreases, particle fragmentation becomes more complete (figs. 4(b) through (d)) until melting and vaporization begin to occur (fig. 4(e)) for $t_1/d = 0.50$. Rear sheets are shown in

figures 4(f) and (g) for structures with t_T/d ratios less than those of the data of figure 2 and show that melting and vaporization become more complete as t_1/d continues to decrease. This trend indicates that, for a given impact velocity, an optimum t_1/d exists that will produce maximum projectile and front-sheet vaporization and/or fragmentation. If the impact velocity is relatively low, then the projectile kinetic energy will be insufficient to vaporize the material and the optimum t_1/d will be determined by the degree of fragmentation. However, for high impact velocities, the energy required to vaporize the material is available and the optimum t_1/d depends upon the degree of material vaporization. Physically, it can be reasoned that the optimum condition exists when the shock waves generated in the front sheet and the projectile have just enough energy when they reach the rear surface of the front sheet and the rear face of the projectile, respectively, to vaporize the last remaining material. Thus, if t_1/d is greater than the optimum value for a given impact velocity, the shock wave in the front sheet decays to the point where it no longer has sufficient energy to vaporize the additional front-sheet material. As t_1/d increases further, the shock wave continues to decay and additional front-sheet material is not vaporized. This phenomenon is evident in figure 4, where the process of fragmentation and vaporization decreases with increasing t_1/d. On the other hand, if t_1/d is less than the optimum value, the shock wave in the projectile is attenuated by the rarefaction wave (reflected shock wave) from the rear surface of the front sheet and by release waves from the free surfaces, and energy is no longer available to vaporize the projectile. When t_1/d becomes sufficiently small, the projectile will not be broken.

Since all the tests in this program were conducted with equally thick front and rear sheets, no attempt was made to determine the optimum t_1/d for different impact velocities. However, figure 4 shows that the optimum t_1/d is less than 0.32 for glass spheres impacting aluminum sheets at 7.85 km/sec. Thus, it seems reasonable to conclude that an optimum double-sheet structure will not consist of two equally thick sheets of material, but will consist of a front sheet designed to provide optimum efficiency (maximum vaporization) and a rear sheet with the remainder of the available mass.

The rear sheets shown in figures 3 and 4 indicate that impacting a relatively thin front sheet at the velocities of these tests corresponds to impacting a thicker front sheet at much higher velocities. Thus, it seems feasible that the effects of impact at meteoric velocities can be simulated by impacts at lower velocities through judicious selections of target materials and thicknesses. It is concluded that, for very large t_1/d, the rear-sheet damage caused by meteoroid impact may very well be represented by the damage in these tests for smaller t_1/d.

The data of these tests enable one to establish the effectiveness of total sheet thickness and a lower limit for the effectiveness of sheet spacing in increasing structural penetration resistance. Fairing curves through the highest velocity data for $t_T/d = 1.00$ and 1.28 show that the ballistic limit varies with the 2.5 power of t_T/d and with at least the square of h/d. These values can be used to express what is thought to be a conservative equation for the ballistic limit of aluminum double-sheet structures impacted at meteoric velocities:

$$B.L. = 0.059(h/d)^{2.0}(t_T/d)^{2.5}, \quad km/sec \tag{1}$$

This equation is plotted in figure 2 as the straight portion of the dashed curves. The slope of the extensions might well be far greater than shown, in which case the exponents of h/d and t_T/d would be greater than shown. If this is the case, equation (1) should be a conservative estimate of the ballistic limit for h/d and t_T/d ratios equal to or greater than those shown in figure 2. Equation (1) is intended only for double-sheet structures that consist of two equally thick sheets of aluminum. It is felt that the situation would be improved considerably if the front sheet were designed to the optimum t_1/d with the remaining available mass in the rear sheet.

Front-Sheet Hole Formation and Mass Loss

The average minimum hole diameter in the front sheet of the structures is presented in figure 5; the ratio of the hole diameter to the projectile diameter, D/d, is plotted versus the square of the impact velocity for various t_1/d. This figure also includes the hole diameter data of reference 1 (filled symbols).

Curves were faired through the data for the t_1/d values that covered the largest velocity range, that is, $t_1/d = 0.50$ and 0.40, to establish the equation

$$D/d = 1.32(t_1/d)^{0.45}v^{1/2} \tag{2}$$

This equation fits the data for all t_1/d less than 0.80. It is thought that equation (2) represents the equilibrium hole growth condition for thin targets impacted at high velocities where front and rear surface effects are negligible and the hole diameter increases primarily as a result of the radially expanding shock wave in the thin sheet. It is thought that targets with t_1/d greater than 0.72 still experience the surface effects characteristic of thicker targets and simply have not attained the equilibrium condition within this velocity range.

Measurements also were made of the front-sheet mass loss. Each target front sheet was weighed before and after it was impacted and the mass loss was determined to an accuracy of 1 percent or better. The mass-loss data are presented in figure 6, where the ratio of front-sheet mass loss to projectile mass, $\Delta M/m$, is plotted versus the impact velocity squared for various t_1/d. Curves faired through the data fit the equation

$$\Delta M/m = 4.1(t_1/d)^2v \tag{3}$$

so that front-sheet mass loss is proportional to the projectile momentum, as was proposed in reference 1. Since the mass loss should vary as the square of the hole diameter times the sheet thickness, that is,

$$\Delta M/m \propto (D/d)^2(t_1/d) \tag{4}$$

it is evident that equations (2) and (3) are compatible with regard to the impact velocity exponent, but that front-sheet mass loss is influenced by an additional small t_1/d effect.

CONCLUDING REMARKS

The present experimental investigation has shown that the ballistic limit of aluminum double-sheet structures increases with increases in both total sheet thickness and sheet spacing. In addition, it is observed that, for a particular ratio of total structural thickness to projectile diameter, the relative effectiveness of sheet spacing in increasing penetration resistance increased with increasing velocity within the velocity range of this test. It is concluded that this effect is the result of melting and vaporization of the projectile and front-sheet spray material and that this trend will continue as material vaporization becomes more dominant. Since the data of these tests are limited to velocities less than 9.0 km/sec, total vaporization obviously has not been achieved. Thus, the highest velocity data presented here have been used to establish the effectiveness of total sheet thickness and a minimum limit on the effectiveness of sheet spacing for two equally thick aluminum sheets. These values have been used to establish what is thought to be a conservative equation for structural ballistic limit:

$$\text{B.L.} = 0.059(h/d)^{2.0}(t_T/d)^{2.5} \qquad (1)$$

Finally, it was observed that, for impacts at a particular velocity, projectile and front-sheet material vaporization and fragmentation increased with decreasing t_1/d. This indicates that, for a given impact velocity, an optimum t_1/d exists that will produce maximum vaporization or fragmentation or both, and will result in the most efficient meteor bumper. The data of these tests show that for an impact velocity of 7.85 km/sec the optimum t_1/d is less than 0.32. Thus, it can be concluded that the double-sheet structure most efficient in resisting penetration should consist of a front sheet designed to the optimum t_1/d with the remaining available mass in the rear sheet.

Ames Research Center
National Aeronautics and Space Administration
Moffett Field, Calif., 94035, Feb. 19, 1968
124-09-15-02-00-21

REFERENCES

1. Nysmith, C. Robert; and Summers, James L.: An Experimental Investigation of the Impact Resistance of Double-Sheet Structures at Velocities to 24,000 Feet Per Second. NASA TN D-1431, 1962.

2. Denardo, B. Pat: Penetration of Polyethylene Into Semi-Infinite 2024-T351 Aluminum Up to Velocities of 37,000 Feet Per Second. NASA TN D-3369, 1966.

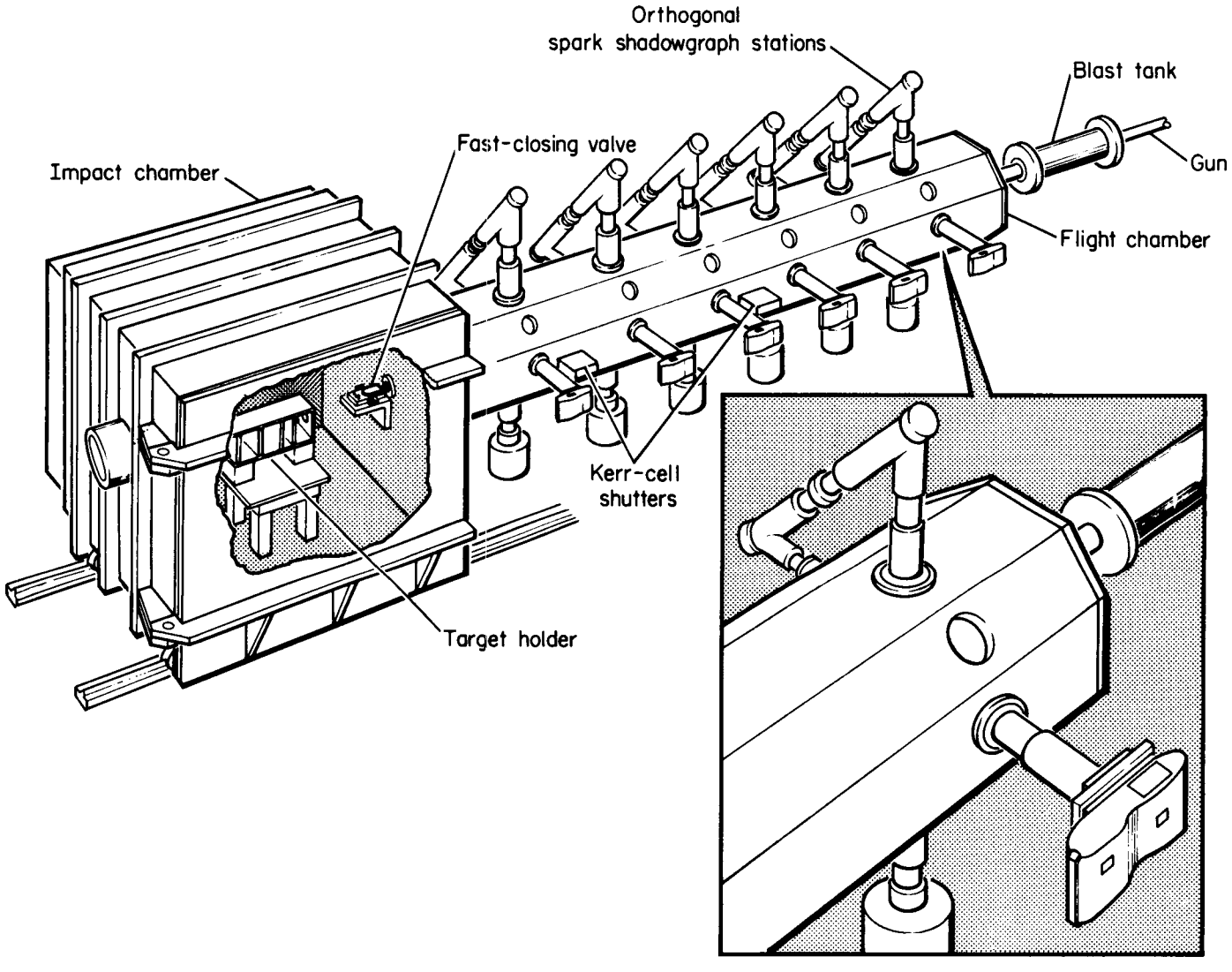

Figure 1.- Range configuration.

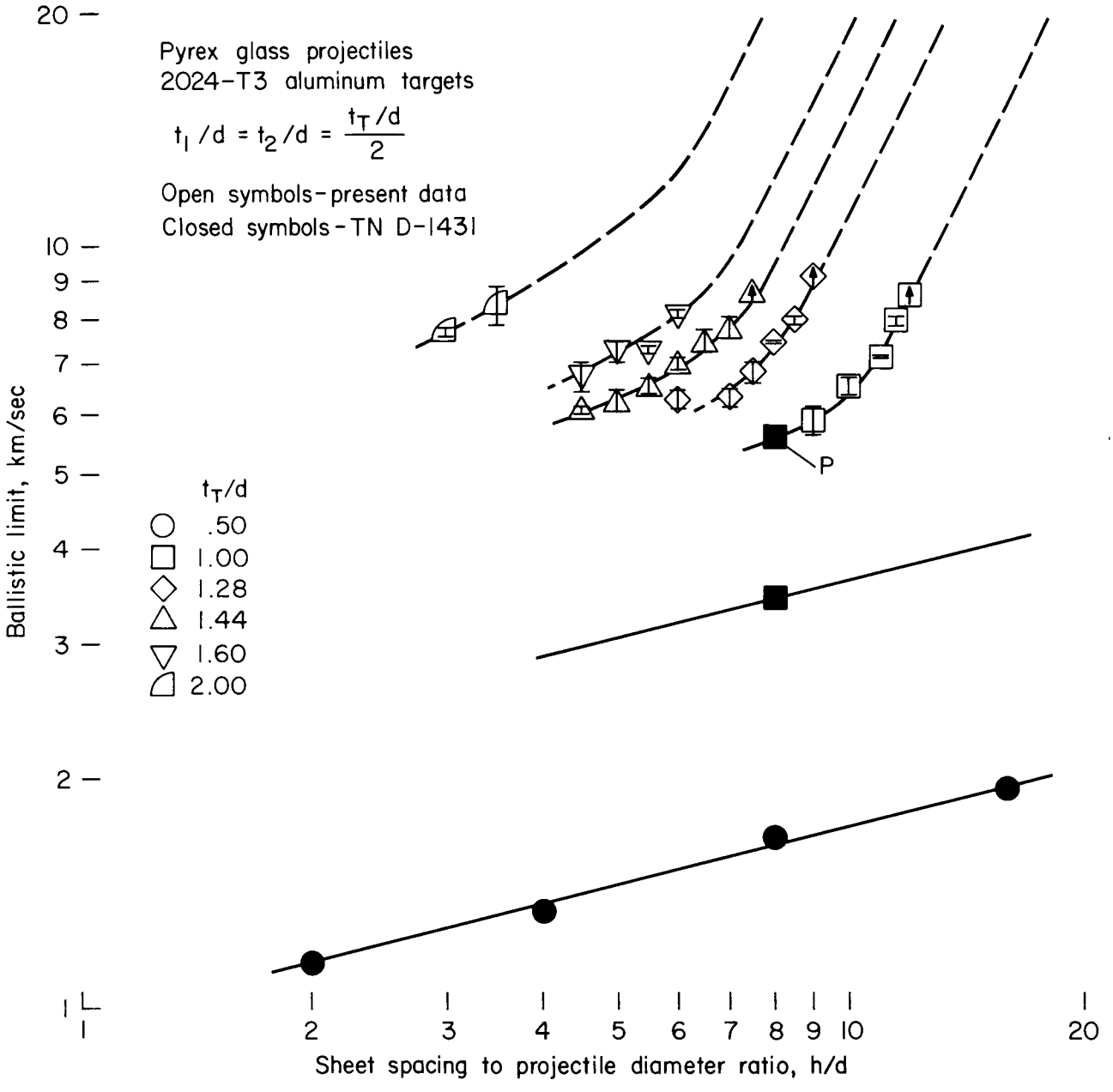

Figure 2.- Ballistic limit of aluminum double-sheet structures.

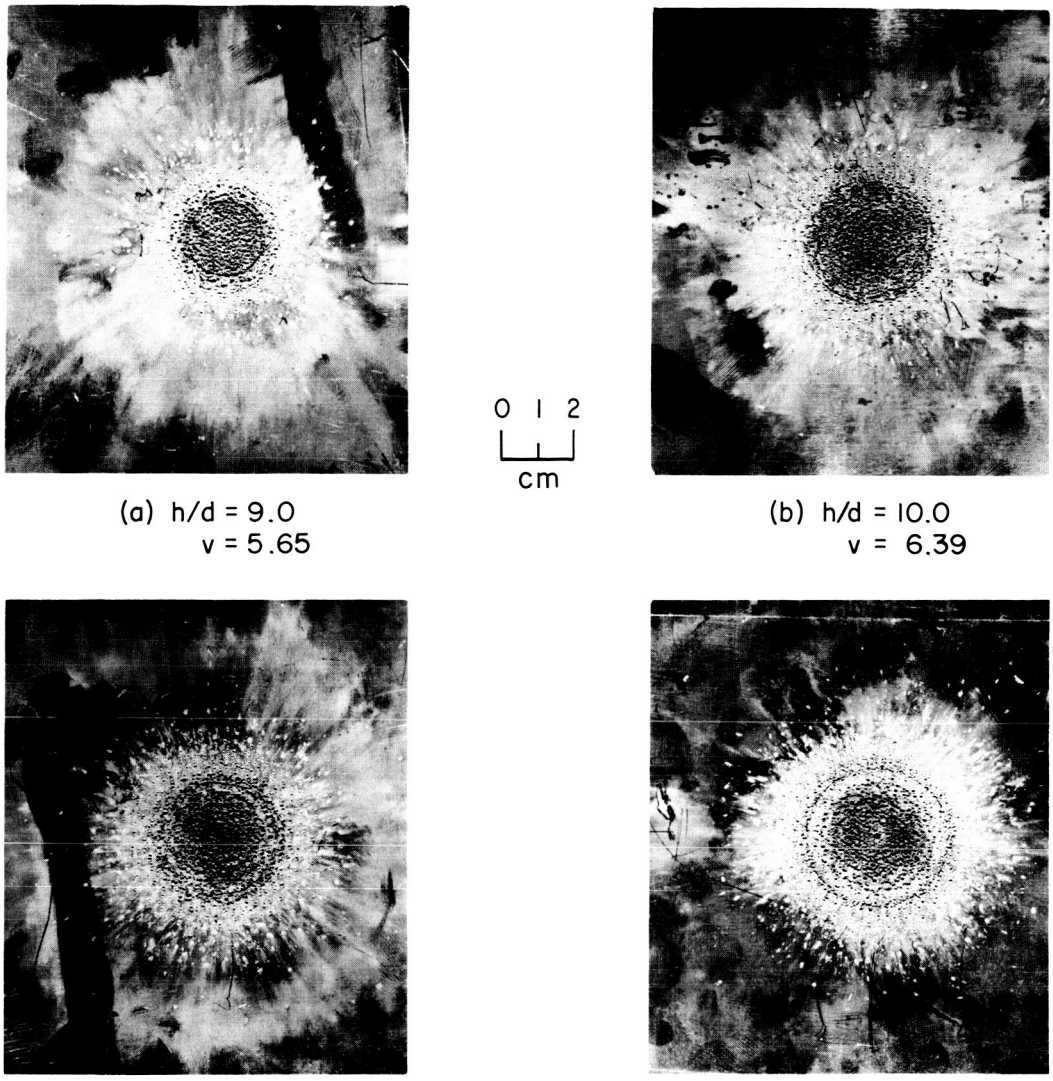

Figure 3.- Variation in rear-sheet damage with impact velocity for $t_1/d = 1.00$.

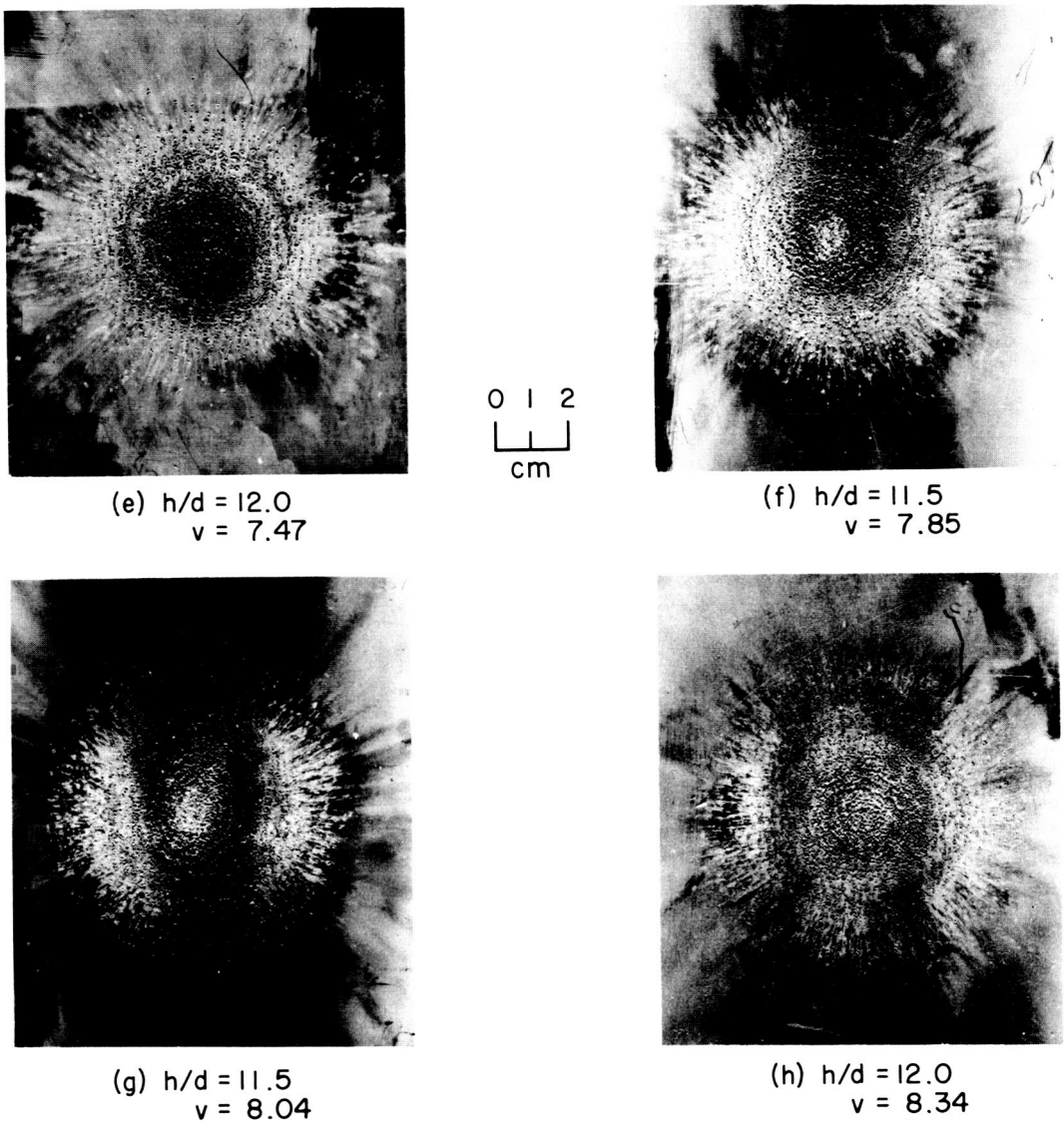

Figure 3.- Concluded.

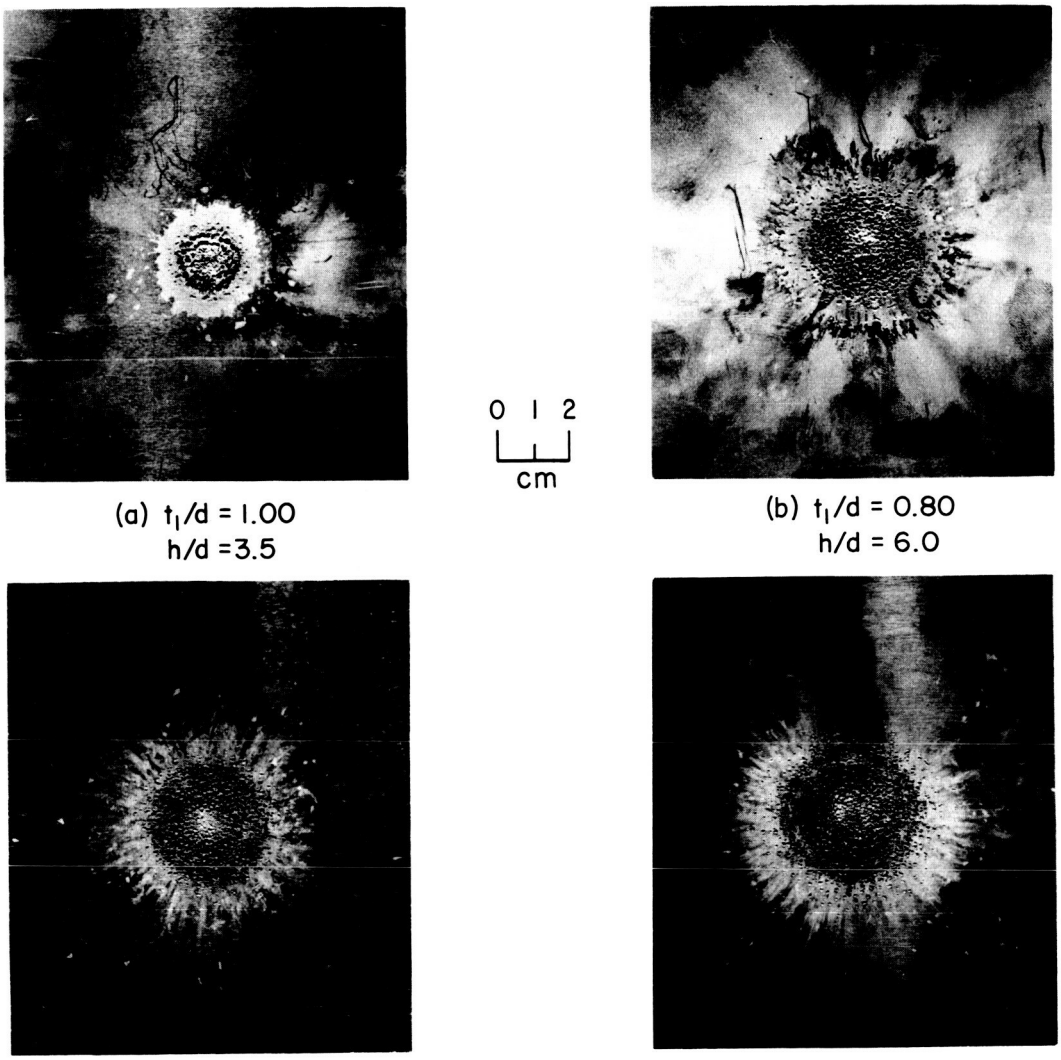

Figure 4.- Variation in rear-sheet damage with t_1/d at an impact velocity of 7.85 km/sec.

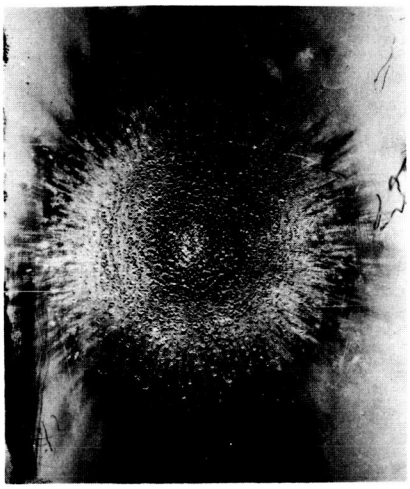

(e) $t_1/d = 0.50$
$h/d = 11.5$

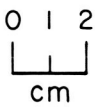

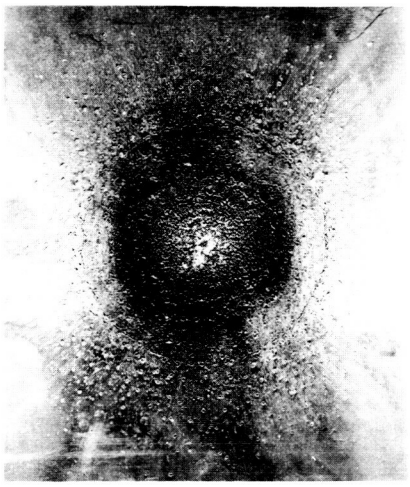

(f) $t_1/d = 0.40$
$h/d = 18.5$

(g) $t_1/d = 0.32$
$h/d = 21.5$

Figure 4.- Concluded.

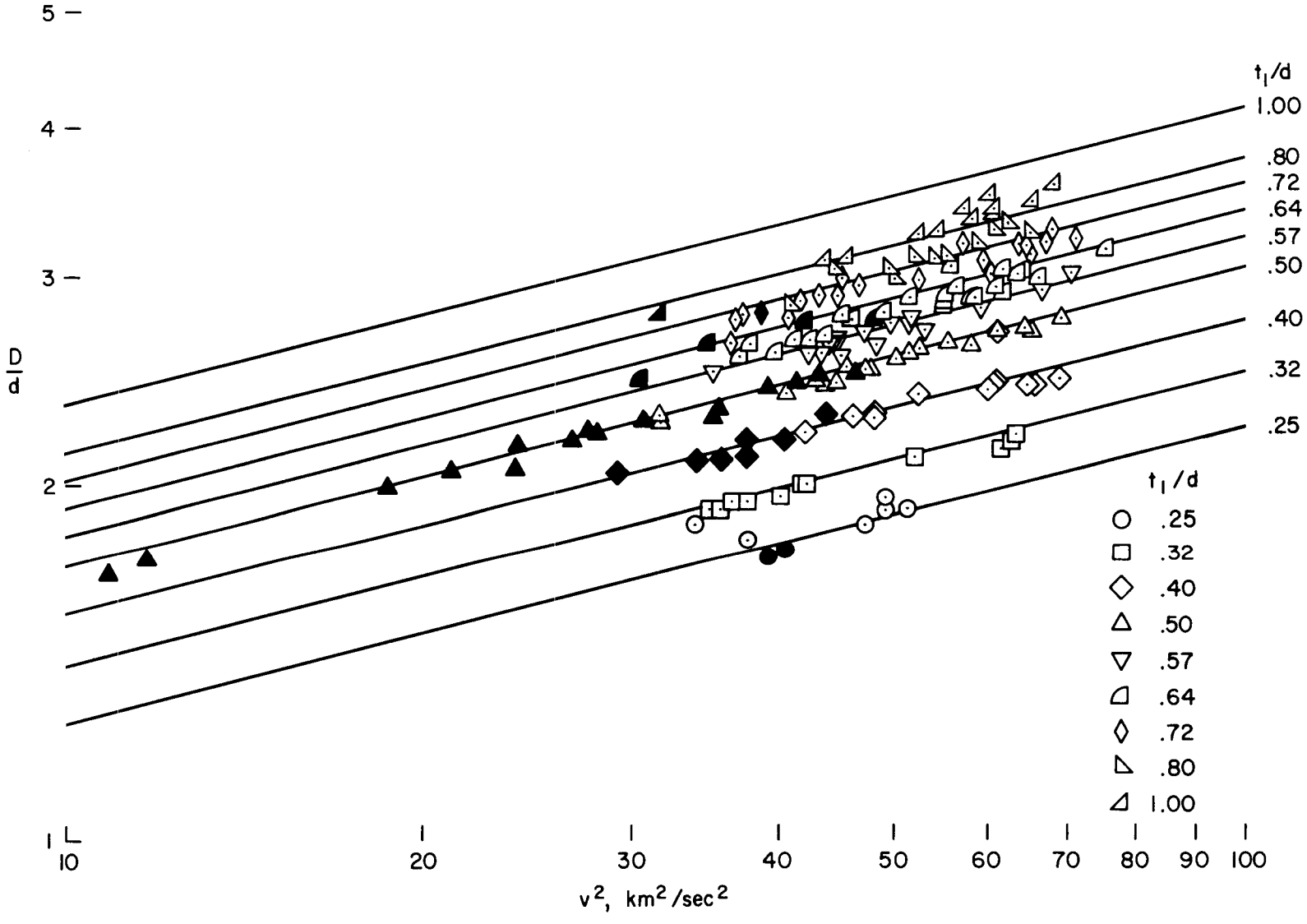

Figure 5.- Variation of the front-sheet hole diameter with impact velocity for various t_1/d ratios.

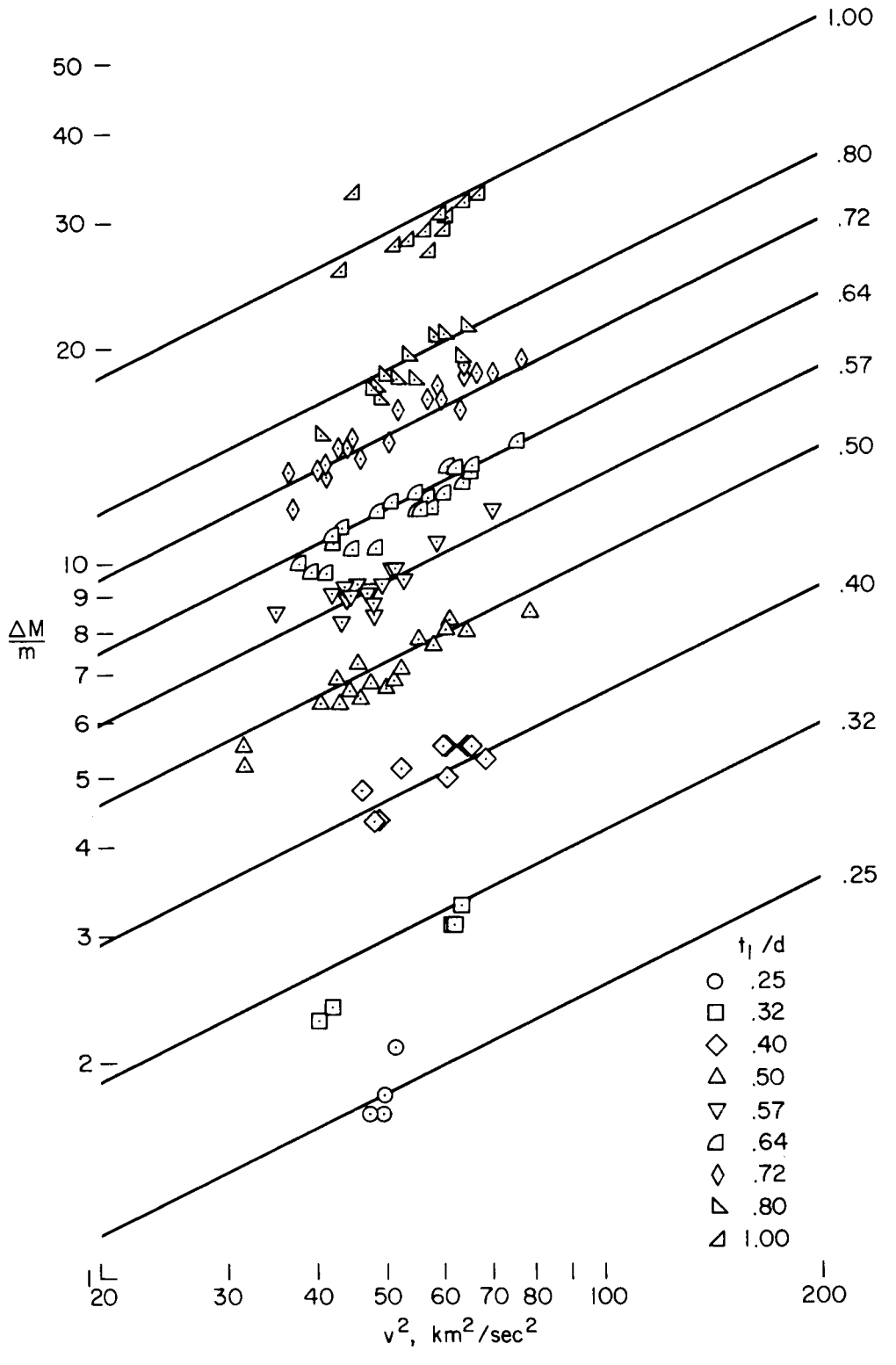

Figure 6.- Variation of the front-sheet mass loss with impact velocity for various t_1/d ratios.

NASA-Langley, 1968 —— 32 A-2831